IOP Publishing — Superconductor Science and Technology
Supercond. Sci. Technol. **31** (2018) 125006 (10pp) https://doi.org/10.1088/1361-6668/aae460

Broad temperature study of RE-substitution effects on the in-field critical current behavior of REBCO superconducting tapes

Shudong Zhang, Shiwei Xu, Ziming Fan, Ping Jiang, Zhichen Han, Gang Yang and Yimin Chen

Key Laboratory for Anisotropy and Texture of Materials, School of Material Science and Engineering, Northeastern University, Shenyang, People's Republic of China

E-mail: yiminchen@mail.neu.edu.cn

Received 20 June 2018, revised 10 September 2018
Accepted for publication 26 September 2018
Published 26 October 2018

Abstract

The critical current behavior of $REBa_2Cu_3O_{7-\delta}$ (REBCO, with RE = Yb, Y, Ho, Dy, Gd, Eu, GdYb, DyY, GdY, EuY, SmY, GdEu, GdSm) superconducting tapes has been systematically studied for the temperature range of 10–77 K, magnetic field range of 0–5 T and field orientation (angle between the field and tape) of 0°–180°. We report that the RE size dependencies of in-field critical current density (J_c) at low temperatures (below 40 K) are significantly different from those at 77 K. In a magnetic field of 1–3 T applied at 77 K, the J_c of REBCO films increases with the RE ionic radius (r). EuBCO film, with the largest r in this study, shows the highest J_c at 77 K in a magnetic field above 1 T, while YbBCO film, with the smallest r, has the lowest J_c at 77 K. At temperatures below 40 K, however, the trend of in-field J_c as a function of r reverses. There are crossovers among the functions of critical current density versus temperature for various RE ions and mixes. RE mixed films such as GdYBCO, EuYBCO, SmYBCO and GdEuBCO exhibit enhanced self-field critical current densities correlating with effective low field random pinning due to their suitable ion size variance. Strongly enhanced pinning by both random and correlated defects has been obtained in GdYbBCO films. Those pinning centers are especially effective at low temperatures. In a magnetic field of 5 T applied at 10 K, GdYbBCO gives the highest critical current density compared with other REBCO films, being 1.9 times greater than GdEuBCO film. This work provides a guideline regarding how to optimize RE ions in REBCO films for given application temperatures and magnetic fields.

Keywords: rare earth substitutions and combinations, REBCO, flux pinning, critical current

(Some figures may appear in colour only in the online journal)

1. Introduction

$REBa_2Cu_3O_{7-\delta}$ (REBCO or RE-123, where RE = rare earth) film based superconducting tapes with high current carrying capacity and mechanical strength have now become commercially available [1–3], after worldwide intensive research for more than two decades. However, their cost/performance ratio is still not satisfactory, especially for applications in a high magnetic field. Therefore, a variety of approaches has been studied to further increase their self-field and in-field critical currents (I_c), including off-stoichiometric compositions [4, 5], rare earth substitutions and combinations [1–3, 6–23], and the addition of $BaZrO_3$ [24–27], $BaSnO_3$ [28, 29], $BaHfO_3$ [23], Gd_2TaO_7 [30], and Ba_2YNbO_6 [31, 32]. Some combined usage of these technologies is expected to substantially improve the performance of REBCO tapes under practical working conditions.

RE substitutions and combinations have attracted great research interest because some REBCO films have superior characteristics to YBCO film. The impacts of RE substitutions include lower processing temperatures and wider processing windows for smaller RE ions [7, 13], higher critical transition temperatures (T_c) for larger RE ions [11, 12], improved surface morphologies for larger RE ions owing to different film growth kinetics, which are essential for the growth of high quality thick films [14, 15], and the possibility of introducing point defects arising from cation exchange between large RE ions and Ba ions [7, 8]. Substituting a Y ion in YBCO with a larger RE ion can enhance the self-field and in-field critical currents at 77 K. This has been proven in GdBCO [2, 3, 16, 17], EuBCO [14, 22, 23] and SmBCO [15, 18] films. MacManus-Driscoll *et al* reported that Y mixed with larger RE ions appeared to be optimum for effective pinning across a wide range of magnetic fields [9]. Chen *et al* reported that the optimized Gd/Y ratio in (Gd,Y) BCO film was about 1 for self-field and low field critical currents [24].

To our knowledge, most existing studies on RE substitutions and combinations in REBCO focused on optimizing their performance at 77 K. There has been no comparative study reported so far on RE substitutions and combinations in REBCO coated conductors at intermediate temperatures of 10–65 K. However, it is in this temperature range where a number of coil-based applications of HTS such as high field magnets, wind generators, marine applications, and industrial motors are being developed. The flux pinning mechanisms can be different at different temperatures [33, 34]. In general, the coherence length is smaller ($\xi^2(T) \approx \xi^2(0)\frac{1}{1-T/T_c}$, $\xi(0)_{ab} = 1.5 \sim 2$ nm) [35] and thermal fluctuation effects are reduced at lower temperatures, allowing weaker and smaller pins to become more prominent. Additionally, the film growth thermodynamics vary among different RE substitutions and combinations, which results in a different distribution of sizes and types of defects (such as stacking faults, threading dislocations, impure phases etc). The optimum densities, sizes and types of defects for effective flux pinning in REBCO films can be different at different temperatures. Therefore, it is essential to study the effects of RE substitutions and combinations on the superconducting properties of REBCO tapes at application temperatures.

The object of this work is to perform a systematic study of the effects of RE substitutions and combinations in REBCO tapes on their in-magnetic-field critical current behavior over a broad temperature range of 10–77 K.

2. Experimental details

REBCO films were deposited by metal–organic chemical vapor depostion (MOCVD) [4, 5, 24, 36, 37] on Hastelloy substrates 65 μm thick and 12 mm wide with ion beam assisted deposition–MgO based buffer architecture [38]. The source for the MOCVD was made by mixing the organometallic tetramethyl heptanedionate compounds for Yb, Y, Ho, Dy, Gd, Eu, Sm, Ba and Cu in tetrahydrofuran solution at appropriate mole ratios. To eliminate deviation caused by the diversity of buffers, the substrates for all REBCO film depositions in the present study were taken from the same buffered tape, which was of a uniform texture profile. The in-plane misalignment angle was within 6.0°–6.6° in the cap layer of the buffer architecture. Many short sample tapes with a variety of RE substitutions and combinations can be processed in a single run in the reel-to-reel MOCVD system to ensure the experiments for all the sample tapes are conducted under the same hardware configurations. The stability of the MOCVD process has been proved in our fabrication of >200 m long REBCO tapes which achieve average critical currents of around 640 A/ 12 mm at 77 K in self-field with a standard deviation less than 5% in 4 m × 4 m I_c measurements [5].

For the comparative study, all REBCO tapes prepared in this work targeted the same film composition, an atomic ratio of RE:Ba:Cu = 1.3:2:3.15 measured by inductively coupled plasma atomic emission spectroscopy (ICP-AES). Such a composition ratio in the film was obtained by adjusting the mole ratio of metals in the precursor for MOCVD. The REBCO film thicknesses in the sample tapes were all around 0.75 μm, ranging from 0.66–0.83 μm measured by cross-sectional scanning electron microscopy (SEM). The REBCO film deposition temperature for every RE or RE combination was optimized for the highest self-field critical current density at liquid nitrogen temperature (J_c(77 K, 0 T)). Such an optimization experiment for each RE or RE combination was repeated at least twice, and the optimum J_c(77 K, 0 T) for a given RE or RE combination was well reproduced with deviations less than 5%.

Inductive critical temperature (T_c) measurements were performed in Quantum Design's MPMS 3 using zero-field cooled magnetization at an applied field of 0.005 T.

Transport critical current (I_c) measurements were conducted at temperatures of 10, 20, 30, 40, 50, 65 and 77 K and in the presence of applied magnetic fields up to 5 T with a standard four-probe method using a field criterion of 1 μV cm^{-1}. The angular dependence of I_c was measured over a range of 180° at various magnetic field strengths and temperatures, but a smaller angle range was taken in I_c measurements at 10 K because of the current limit of the I_c measurement system.

Both a whole width (12 mm) sample and a bridge sample from each tape were used in the I_c measurements. The bridges prepared by the wet etching method were about 1.3 mm wide and about 5 mm long. Samples were about 52 mm long, so as to fit in the space in the cryostat of I_c the measurement system. The I_cs of the tapes at temperatures of 50 K and below were obtained by measuring the bridge samples, while I_cs at 77 K and 65 K were obtained directly from measurements on the whole width samples, because I_c for the whole width of 12 mm at the lower temperature could exceed the system's up-limit of 400 A.

3. Results and discussion

Table 1 summarizes the superconducting tapes prepared for this study. The composition ratios of RE:Ba:Cu by ICP-AES for REBCO films are all around 1.3:2:3.15, as seen in the second column of table 1. Such an off-stoichiometric composition ratio in the film can give better superconducting properties [4, 5, 25] than a 1:2:3 stoichiometric ratio does.

Table 1. Properties of REBCO tapes studied.

RE[b]	RE:Ba:Cu or RE1:RE2: Ba:Cu	Optimum deposition temperature (°C)	J_{c_min} (MA cm^{-2})[a]				
			77 K, 0 T	77 K, 3 T	20 K, 0 T	20 K, 3 T	20 K, 5 T
Yb	1.33: 2: 3.20	760	1.60	0.01	24.76	6.82	5.33
Ho	1.26: 2: 3.19	795	2.60	0.09	25.33	6.63	5.09
GdYb	0.63: 0.63: 2: 3.10	805	2.56	0.08	28.87	8.20	5.92
Y	1.28: 2: 3.10	795	2.63	0.07	29.52	8.29	5.92
DyY	0.63: 0.63: 2: 3.19	805	2.54	0.09	27.42	7.18	5.51
Dy	1.26: 2: 3.20	815	2.63	0.10	23.28	5.50	3.98
GdY	0.64: 0.64: 2: 3.20	815	3.52	0.11	27.89	5.57	4.18
EuY	0.64: 0.64: 2: 3.10	825	3.76	0.12	29.24	5.38	3.76
SmY	0.62: 0.62: 2: 3.10	825	3.69	0.07	25.50	4.77	3.44
Gd	1.30: 2: 3.20	825	3.03	0.10	22.45	4.99	3.36
GdEu	0.63: 0.63: 2: 3.10	825	3.69	0.13	25.21	4.77	3.38
GdSm	0.64: 0.64: 2: 3.15	825	3.22	0.10	23.04	4.62	3.31
Eu	1.30: 2: 3.18	835	3.52	0.14	23.33	5.45	3.69

[a] J_{c_min} in the table is the minimum value of field-orientation dependent critical current density.
[b] REs and RE combinations for REBCO tapes are listed in the order of RE size or average RE ionic radius.

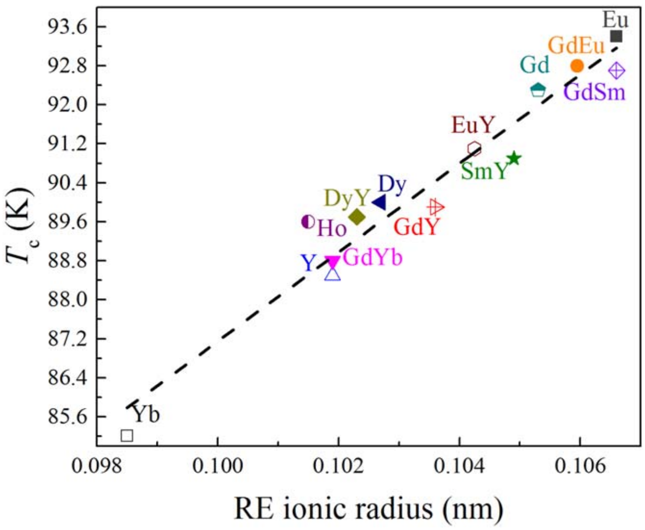

Figure 1. Critical temperature versus average RE ionic radius for REBCO superconducting tapes.

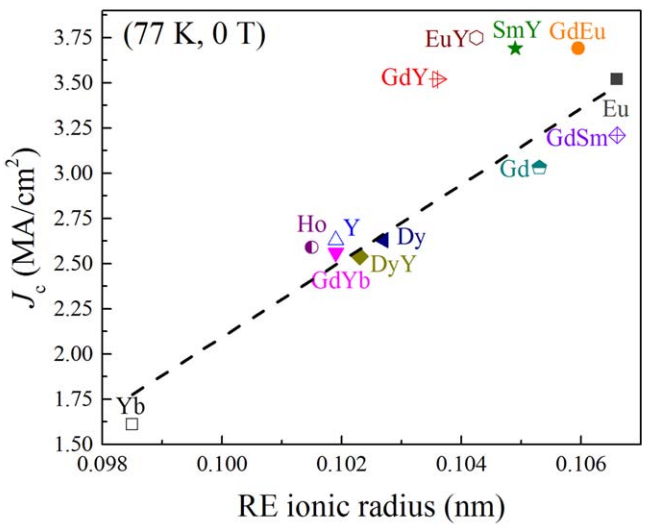

Figure 2. Critical current density at 77 K in the self-field versus average RE ionic radius for REBCO superconducting tapes.

The optimum deposition temperature displayed in the third column shows an increasing trend with the average RE ionic radius. It can be associated with RE size dependence of the decomposition temperature of RE-123. The individually optimized MOCVD condition for every RE composition, and the consistency of RE:Ba:Cu ratios for all the samples, provide the foundations for the comparison of various REBCO tapes to investigate the RE effects.

3.1. RE effects on T_c and self-field J_cs of REBCO tapes at different temperatures

Figure 1 shows the critical temperature (T_c) as a function of the RE ionic radius (r). For REBCO films with RE combinations, the average radius of RE ions is used. The change of T_c from 85.2 K to 93.4 K with increasing r from 0.0985 nm for Yb to 0.1066 nm for Eu shows a near-linear trend, which is overall in good agreement with early studies of bulk materials [11, 12]. It has been proved that the r effect on T_c in mono-RE REBCO films originates from the strain-induced charge redistribution between the charge reservoir and the CuO_2 plane [11] and correlates directly with separation of the CuO_2 plane [12, 39] due to the changes of lattice parameters of RE substitutions. The T_c of binary RE films fit well to the trendline, evidencing the formation of a uniform mixing RE-123 phase.

The J_c behavior of REBCO film at 77 K may be influenced by its T_c. The critical current density at 77 K in the self-field increases with the RE ionic radius, as illustrated in figure 2. However, there is no such trend in RE size dependence of J_c at 20 K in the self-field, as seen in figure 3.

REBCO films with binary RE ions, such as GdYBCO, EuYBCO, SmYBCO and GdEuBCO, exhibit enhanced J_c in the self-field at 77 K, which may be attributed to low field

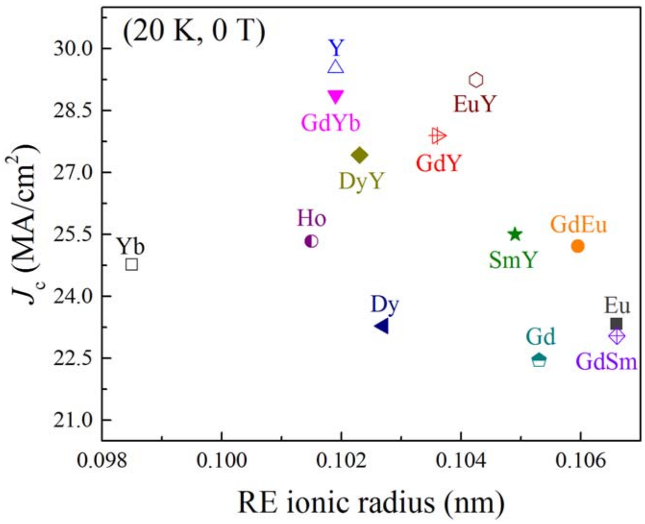

Figure 3. Critical current density at 20 K in the self-field versus average RE ionic radius for REBCO superconducting tapes.

random pinning due to their suitable ion size variance [6–10, 20, 21].

The data in the sixth column of table 1 and in figure 3 suggests that the combination of a small RE ion (Yb or Y) with a large RE ion (Gd, Eu, Sm or Dy) results in a high J_c in a self-field at a low temperature (20 K). While EuY-123 and GdEu-123 films show the highest self-field J_c at 77 K, Y-123 has the highest self-field J_c at 20 K.

3.2. RE effects on J_cs of REBCO tapes in applied magnetic fields at different temperatures

The magnetic field orientation dependencies of J_c of REBCO tapes in magnetic fields of 1 T applied at 77 K, 3 T applied at 77 K, 65 K, 50 K, 40 K, 30 K and 20 K and 5 T applied at 10 K are displayed in figure 4. In a magnetic field of 1–3 T applied at 77 K, EuBCO and GdEuBCO films exhibit the highest J_{c_min} while the performances of YbBCO, GdYbBCO and YBCO films are relatively poor. YbBCO has the lowest J_c at 77 K, being 1/5 of the value of EuBCO in 1 T and 1/14 of the value of EuBCO in 3 T. No significant *c*-peaks (peaks at 0° in J_c as a function of the angle between the magnetic field and tape normal) are observed under this temperature condition.

However, their levels change over in the J_c comparison as the temperature lowers. At 20 K, GdYbBCO and YBCO films have the best J_c behavior. At (20 K, 3 T), the J_c of YbBCO film exceeds those of other films except GdYbBCO, YBCO and DyYBCO, even though YbBCO has the lowest J_c at 77 K.

It is noticeable in figure 4 that a prominent broad peak centered on the $B//c$ direction appears in the J_c curve for GdYbBCO tape at 65 K and below, though there is not such an outstanding '*c*-peak' seen for GdYbBCO tape at 77 K. The emergence of strong *c*-peak could be an indication of additional pinning mechanisms coming into play when the temperature drops from 77 K to a low temperature.

The enhancement of the *c*-peak in angular dependent critical current density at 40–65 K is also significant for YBCO, HoBCO and DyYBCO tapes.

At (30 K, 3 T), the *c*-peak for GdYbBCO tape is still high. The two-dimensional pinning [24] in the GdYbBCO film keeps it strong over a broad temperature range. This behavior is similar to that of GdYBCO film with very high level Zr addition [26]. When the temperature drops to 10 K, the *c*-peak is flattened. This could be interpreted as more random oriented pinning defects taking effect at low temperatures.

At (10 K, 5 T), GdYbBCO film gives the highest J_{c_min} among all the REBCO films, being 1.9 times the value for GdEuBCO, even though the latter has the highest J_c at 77 K.

Magnetic field dependencies of critical current density for REBCO tapes at 65 K and 20 K with fields perpendicular to the tape are shown in figures 5 and 6, respectively. At 65 K, GdYbBCO, YBCO and HoBCO tapes show enhanced J_c performance in higher magnetic fields. The different in-field performances among various REBCO tapes result in some crossovers in J_c–B plots. At 20 K, GdYbBCO and YBCO tapes show high J_c in the whole field range of 1–5 T.

Figure 7 shows J_{c_min} as a function of temperature for REBCO superconducting tapes in a magnetic field of 3 T. J_{c_min} in the figures takes the minimum value in angular dependent J_c given in figure 4. As seen in figure 7, GdYbBCO and YBCO superconducting tapes are advantageous over the others at temperatures below 30 K, but GdYbBCO tape is the best at temperatures below 20 K.

There are some crossovers among the J_{c_min}–T curves for REBCO tapes with different RE. At a low temperature, the J_c difference between these tapes can be very large. These findings clearly emphasize the importance of optimizing the RE element or combination of elements in REBCO coated conductors for practical operating conditions.

From the trends of figures 6 and 7, we predict that GdYbBCO will perform even better in higher magnetic fields (>5 T) at low temperatures.

Figure 8 exhibits trends of J_{c_min} versus average RE ionic radius (r) for various REBCO tapes in magnetic fields of 1 T applied at 77 K, 3 T applied at 77 K, 65 K, 50 K, 40 K, 30 K and 20 K, and 5 T applied at 20 K. As seen in the figure, J_{c_min} at (77 K, 1 T) and (77 K, 3 T) increases with the RE ionic radius. The most interesting new finding here is, however, that such a trend vanishes at 50 K and reverses at further lower temperatures. The trend of J_{c_min} versus r changes with temperature. The REBCO tapes with a small RE ionic radius are advantageous when being used at low tempereaures and high magnetic fields. This finding provides a guideline for choosing RE elements or a combination of elements in REBCO coated conductors for practical application conditions.

Comparing figure 8 with figure 1, one can see that binary RE films, GdYBCO, EuYBCO, SmYBCO and GdEuBCO, showing higher critical current density in the self-field at 77 K are advantageous in magnetic fields of 1 T and 3 T. This proves that the pinning with ion size variance in the binary

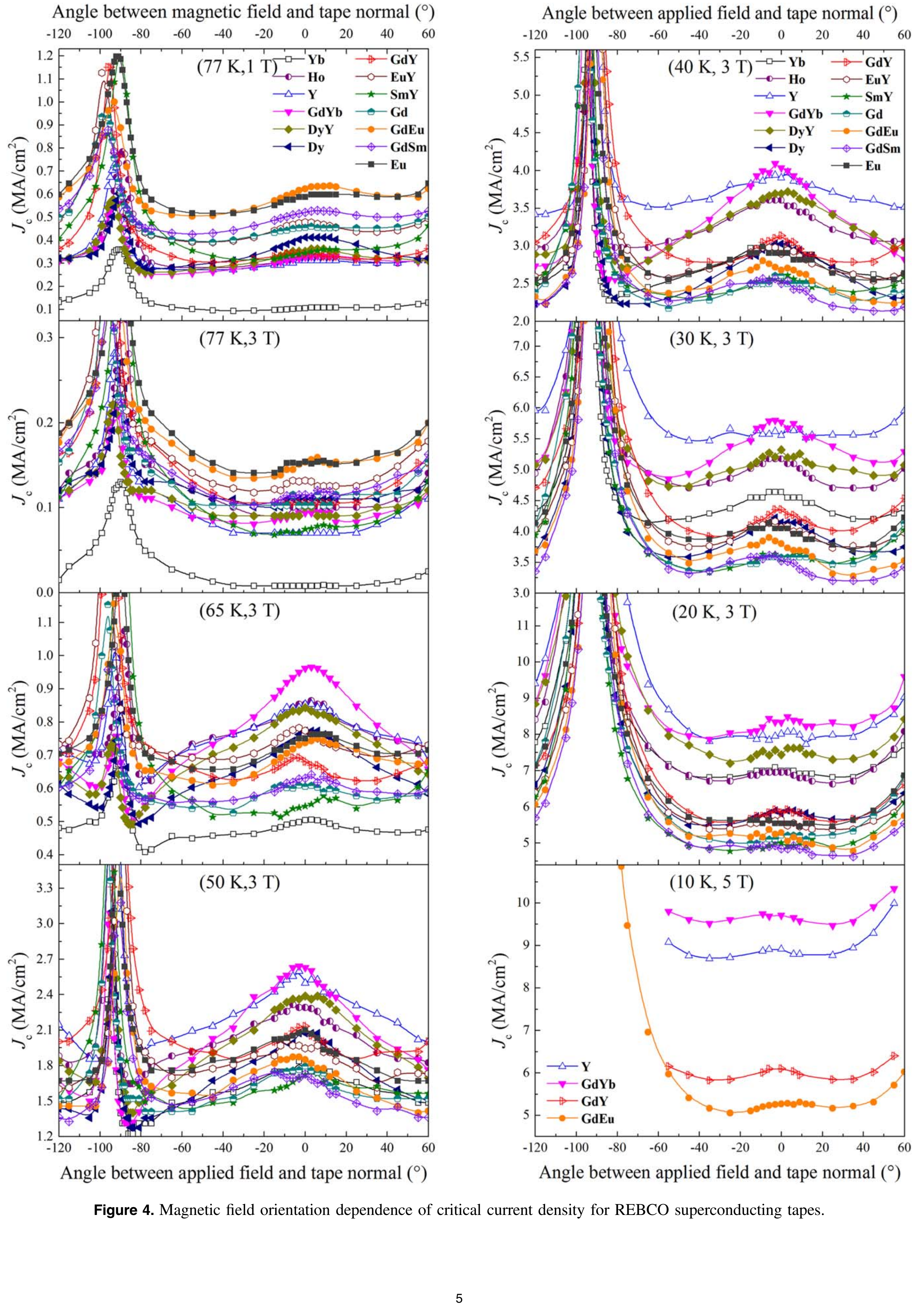

Figure 4. Magnetic field orientation dependence of critical current density for REBCO superconducting tapes.

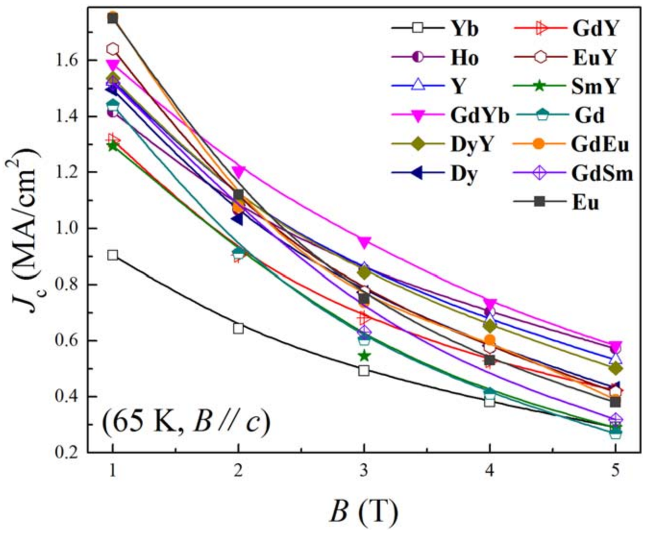

Figure 5. Critical current density versus magnetic field applied perpendicular to the surface for REBCO tapes at 65 K.

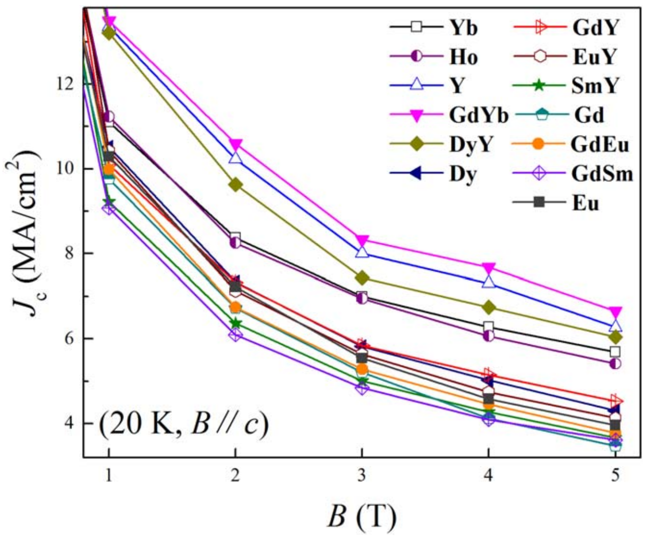

Figure 6. Critical current density versus magnetic field applied perpendicular to the surface for REBCO tapes at 20 K.

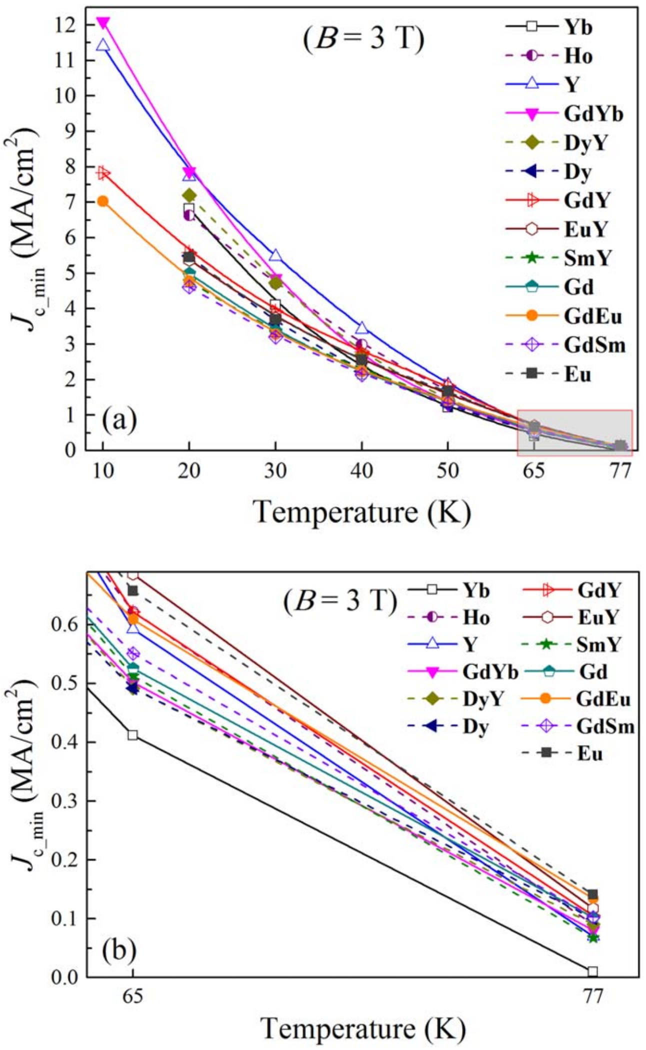

Figure 7. Comparison of REBCO tapes on temperature dependence of critical current density in a magnetic field of 3 T. (a) 10–77 K range, (b) closer view of 65–77 K.

rare earth films is effective only in the self-field and low magnetic fields.

The J_c data obtained in the present study suggests that EuYBCO, GdYBCO and SmYBCO coated conductors are good choices for applications in self-fields or low magnetic fields of <0.1 T at temperatures of 40–77 K. EuBCO and GdBCO are of high J_c in a magnetic field of 0.1–3 T applied at 65–77 K. GdEuBCO suits applications in 0–1 T at 65–77 K. YBCO is superior to others in 3–5 T at 20–40 K. In 3–5 T at 10–20 K, GdYbBCO tapes are applicable. Interesting follow-up works include extending the study to magnetic fields above 5 T and temperatures down to 4 K.

3.3. RE effects on the microstructures of REBCO films

Shown in figure 9 are the SEM surface morphologies of REBCO films studied in this work. The images in the figure are labeled with REBCO names. The surface of the REBCO films with larger average RE ionic radii are cleaner, smoother and denser with fewer particulates, which can probably be attributed to their relatively higher deposition temperature and consequently more complete chemical reactions between metallic compounds. More outer-growth grains are seen on the surfaces of REBCO films with smaller RE ionic radii. Identified by shapes [5], they include *c*-axis tilted grains and 45° rotated misaligned grains. The surface morphologies suggest that it is easier to deposit high quality thick REBCO films with lager RE ionic radii.

There was almost no difference among x-ray diffraction (XRD) ω scans at (005) and φ scans at (103) for the REBCO films in this study. The full widths at half maximum are all about 1° in the ω scan peaks and 2.5° in the φ scan peaks. The XRD θ–2θ scans for the REBCO tapes are shown in figure 10. The most significant difference among the XRD θ–2θ scans is in their intensities of RE_2O_3 (400) peaks. The intensities of the RE_2O_3 (400) peaks is higher in REBCO films with smaller r, and reduces with increasing r. RE_2O_3 related peaks can hardly

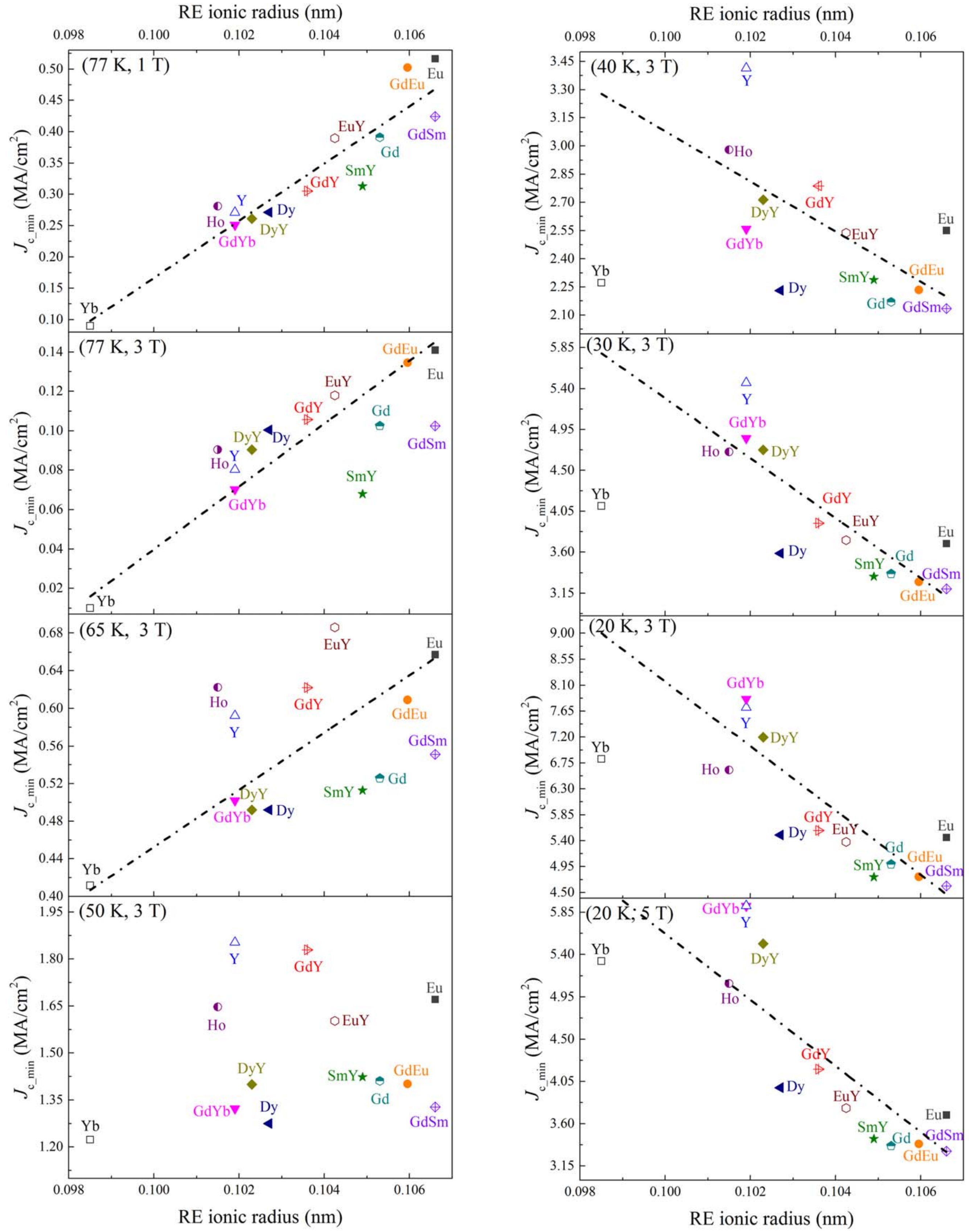

Figure 8. J_{c_min} versus RE ionic radius in magnetic fields of 1 T applied at 77 K, 3 T applied at 77 K, 65 K, 50 K, 30 K, 40 K and 20 K, and 5 T applied at 20 K.

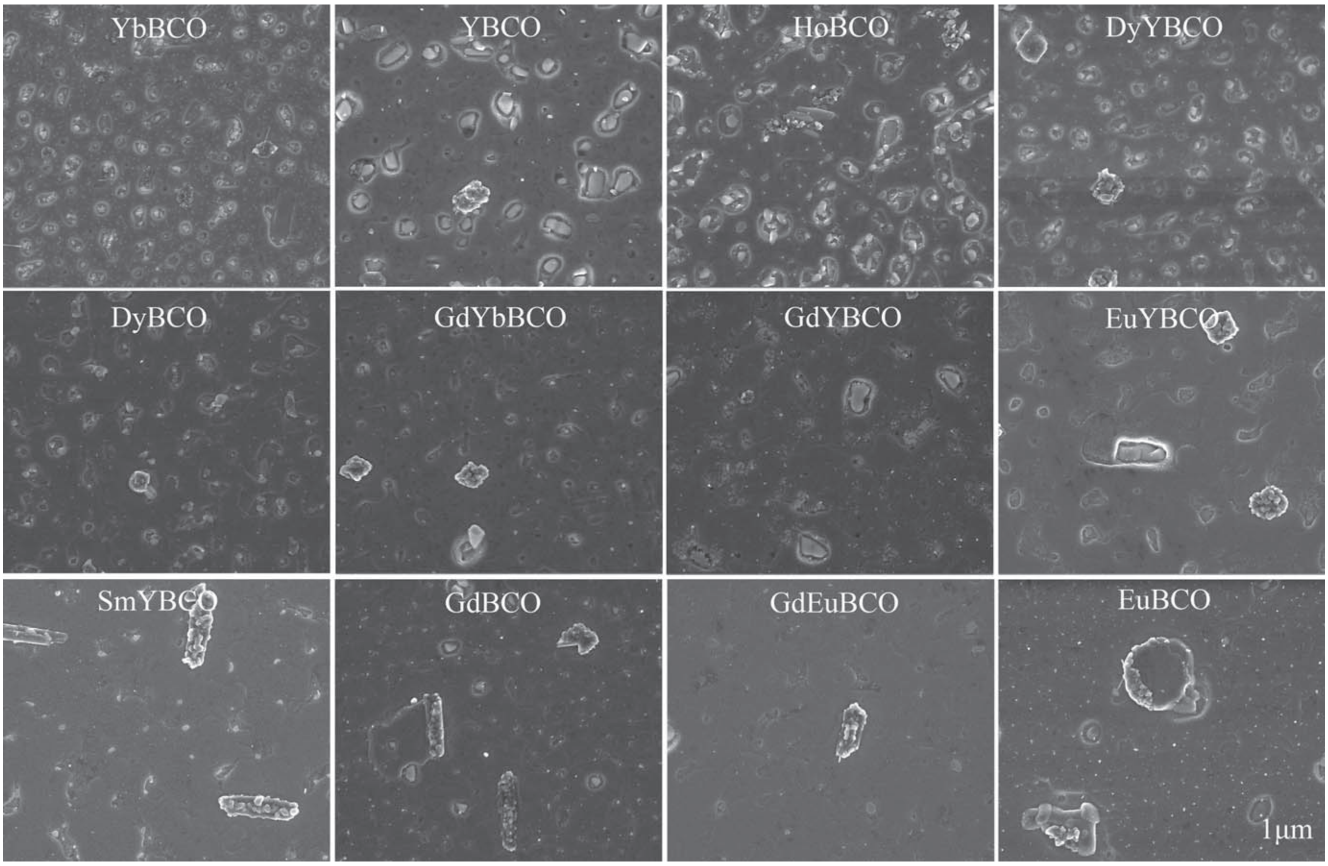

Figure 9. SEM surface morphologies of REBCO films.

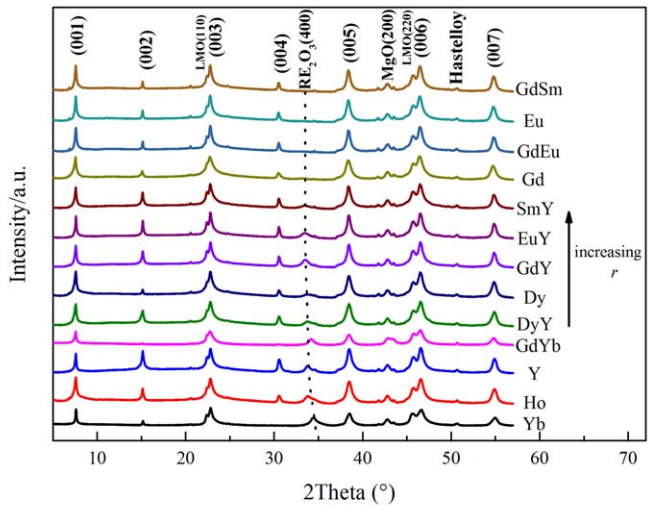

Figure 10. Comparison of XRD θ–2θ scanning patterns of the REBCO tapes.

be observed in XRD θ–2θ scans for GdSmBCO, EuBCO, GdEuBCO, GdBCO films. The RE_2O_3 precipitates in REBCO films with a large r are unlikely to form as good a crystal structure as that formed in REBCO films with a small r. The possibility of large RE ions occupying Ba sites may also contribute to reducing the amount of RE_2O_3 crystallites.

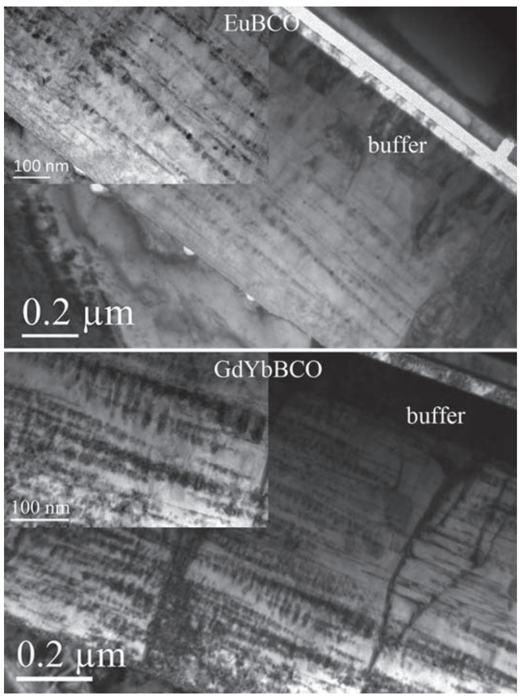

Figure 11. The cross-sectional TEM image of EuBCO and GdYbBCO tapes.

The cross-sectional transmission electron microscopy (TEM) images given in figure 11 confirm that the density of RE_2O_3 crystallites in planar structures in the EuBCO film is not as high as in the GdYbBCO and GdYBCO films [24].

The TEM cross-sectional image of GdYbBCO tape in figure 11 shows a high density of vertical and horizontal aligned defects. We believe that these nanoscale defects may be responsible for the outstanding performance of GdYbBCO tapes in high magnetic fields at low temperatures. Further analysis of the microstructure and study of the formation mechanism of these defects is under way.

4. Conclusions

The present systematic study of RE effects on the critical current behavior of REBCO superconducting tapes over a temperature range of 10–77 K and a magnetic field range of 0–5 T has reached the following conclusions or new findings.

(1) The optimum RE element or combination of elements in RE-123 superconducting tape is different for different application temperatures and magnetic fields.
(2) Eu-123 and GdEu-123 tapes exhibit the highest J_c in a magnetic field of 1–3 T applied at 77 K.
(3) GdYb-123 tape has the highest J_c at a low temperature (20 K and below) in a high magnetic field (5 T or above).
(4) The RE effect on J_c can be very significant. At (10 K, 5 T), the J_c of the GdYb-123 film is 1.9 times that of the GdEu-123 film, while at (77 K, 1 T), the J_c of the GdYb-123 film is only half that of the GdEu-123 film.
(5) RE mixed films such as GdY-123, EuY-123, SmY-123 and GdEu-123 exhibit enhanced J_c in the self-field at 77 K.
(6) At 77 K, the self-field J_c of REBCO film tends to increase with the RE ionic radii. At a low temperature below 65 K, however, there is no such trend.
(7) In a high magnetic field (3 T and above) applied at low temperatures (40 K and below), the J_c of REBCO film tends to decrease with the RE ionic radii.

Acknowledgments

This work was supported in part by the China Fundamental Research Funds for the Central Universities (grant N170208023).

ORCID iDs

Yimin Chen https://orcid.org/0000-0002-6063-9418

References

[1] Zhang Y F, Lehner T F, Fukushima T, Sakamoto H and Hazelton D W 2014 *IEEE Trans. Appl. Supercond.* **24** 7500405
[2] Iijima Y *et al* 2015 *IEEE Trans. Appl. Supercond.* **25** 6604104
[3] Lee J H, Lee H J, Lee J W, Choi S M, Yoo S I and moon S H 2014 *Supercond. Sci. Technol.* **27** 044018
[4] Fan Z M, Qi Y, Gu H W and Chen Y 2015 *IEEE Trans. Appl. Supercond.* **25** 6601905
[5] Jiang P, Zhang S D, Fan Z M, Xu S W, Zhang S, Ge M, Gu H W and Chen Y 2017 *IEEE Trans. Appl. Supercond.* **27** 6600405
[6] MacManus-Driscoll J L *et al* 2004 *Appl. Phys. Lett.* **84** 5329–31
[7] Jia Q X, Maiorov B, Wang H, Lin Y, Foltyn S R, Civale L and MacManus-Driscoll J L 2005 *IEEE Trans. Appl. Supercond.* **15** 2723–6
[8] MacManus-Driscoll J L *et al* 2005 *Appl. Phys. Lett.* **86** 032505
[9] MacManus-Driscoll J L, Maiorov B, Durrell J, Foltyn S, Jia Q X, Civale L, Wang H, Kursumovic A and Peterson D E 2006 *Supercond. Sci. Technol.* **19** S55–9
[10] Zhou H, Maiorov B, Wang H, MacManus-Driscoll J L, Holesinger T G, Civale L, Jia Q X and Foltyn S R 2008 *Supercond. Sci. Technol.* **21** 025001
[11] Lin J G, Huang C Y, Xue Y Y, Chu C W, Cao X W and Ho J C 1995 *Phys. Rev.* B **51** 12900–3
[12] Varela M, Arias D, Sefrioui Z, Leon C, Ballesteros C, Pennycook S J and Santamaria J 2002 *Phys. Rev.* B **66** 134517
[13] MacManus-Driscoll J L, Alonso J A, Wang P C, Geballe T H and Bravman J C 1994 *Physica* C **232** 288–308
[14] Jia Q X *et al* 2003 *Appl. Phys. Lett.* **83** 1388–90
[15] Jia Q X, Foltyn S R, Coulter J Y, Smith J F and Maley M P 2002 *J. Mater. Res.* **17** 2599–603
[16] MacManus-Driscoll J L, Bianchetti M, Kursumovic A, Kim G, Jo W, Wang H, Lee J H, Hong G W and Moon S H 2014 *APL Mater.* **2** 086103
[17] Fujita S, Daibo M, Igarashi M, Kikutake R, Kakimoto K, Iijima Y, Itoh M and Saitoh T 2014 *J. Phys.: Conf. Ser.* **507** 022007
[18] Kim H S, Oh S S, Ha H S, Youm D, Moon S H, Kim J H, Dou S X, Heo Y U, Wee S H and Goyal A 2014 *Sci. Rep.* **4** 4744
[19] Foltyn S R, Civale L, Macmanus-Driscoll J L, Jia Q X, Maiorov B, Wang H and Maley M 2007 *Nat. Mater.* **6** 631–42
[20] Goswami R, Haugan T J, Barnes P N, Spanos G and Holtz R L 2010 *Physica* C **470** 318–22
[21] Haugan T J, Campbell T A, Pierce N A, Locke M F, Maartense I and Barnes P N 2008 *Supercond. Sci. Technol.* **21** 025014
[22] Yoshida T, Ibi A, Takahashi T, Yoshizumi M, Izumi T and Shiohara Y 2014 *Physica* C **504** 42–6
[23] Yoshida T, Ibi A, Takahashi T, Yoshizumi M, Izumi T and Shiohara Y 2015 *Physica* C **518** 54–7
[24] Chen Y, Selvamanickam V, Zhang Y F, Zuev Y, Cantoni C, Specht E, Paranthaman M P, Aytug T, Goyal A and Lee D 2009 *Appl. Phys. Lett.* **94** 062513
[25] Chen Y, Shi T, Guevara A P, Zhang Y X, Yao Y, Kesgin I and Selvamanickam V 2011 *IEEE Trans. Appl. Supercond.* **21** 3166–70
[26] Selvamanickam V *et al* 2013 *Supercond. Sci. Technol.* **26** 035006
[27] Xu A X *et al* 2015 *IEEE Trans. Appl. Supercond.* **25** 6603105
[28] Varanasi C V, Burke J, Brunke L, Wang H, Lee J H and Barnes P N 2008 *J. Mater. Res.* **23** 3363–9
[29] Varanasi C V, Burke J, Wang H, Lee J H and Barnes P N 2008 *Appl. Phys. Lett.* **93** 092501
[30] Harrington S A, Durrell J H, Maiorov B, Wang H, Wimbush S C, Kursumovic A, Lee J H and MacManus-Driscoll J L 2009 *Supercond. Sci. Technol.* **22** 022001
[31] Ercolano G, Bianchetti M, Wimbush S C, Harrington S A, Wang H, Lee J H and MacManus-Driscoll J L 2011 *Supercond. Sci. Technol.* **24** 095012

[32] Rizzo F *et al* 2016 *APL Mater.* **4** 061101
[33] Xu A X, Braccini V, Jaroszynski J, Xin Y and Larbalestier D C 2012 *Phys. Rev.* B **86** 115416
[34] Xu A X, Jaroszynski J, Kametani F and Larbalestier D 2015 *Appl. Phys. Lett.* **106** 052603
[35] Wee S H, Zuev Y L, Cantoni C and Goyal A 2013 *Sci. Rep.* **3** 2310
[36] Chen Y 2008 High throughput MOCVD process for manufacturing high temperature superconductor wires *Applied Physics in the 21st Century* ed C Xin (Trivandrum: Research Signpost)
[37] Chen Y and Selvamanickam V 2007 Metal organic chemical vapor deposition for the fabrication of YBCO superconducting tapes *Flux Pinning and AC Loss Studies on YBCO Coated Conductors* ed M Paranthaman and V Selvamanickam (New York: Nova)
[38] Chen Y *et al* 2008 *Mater. Res. Soc. Online Proc.* **1009E** 1009 II01–02
[39] Varela M, Sefrioui Z, Arias D, Navacerrada M A, Lucia M, Lopez de la Torre M A, Leon C, Loos G D, Sanchez-Quesada F and Santamaria J 1999 *Phys. Rev. Lett.* **83** 3936–9